Article

Cell Reports

PTENα Modulates CaMKII Signaling and Controls Contextual Fear Memory and Spatial Learning

Graphical Abstract

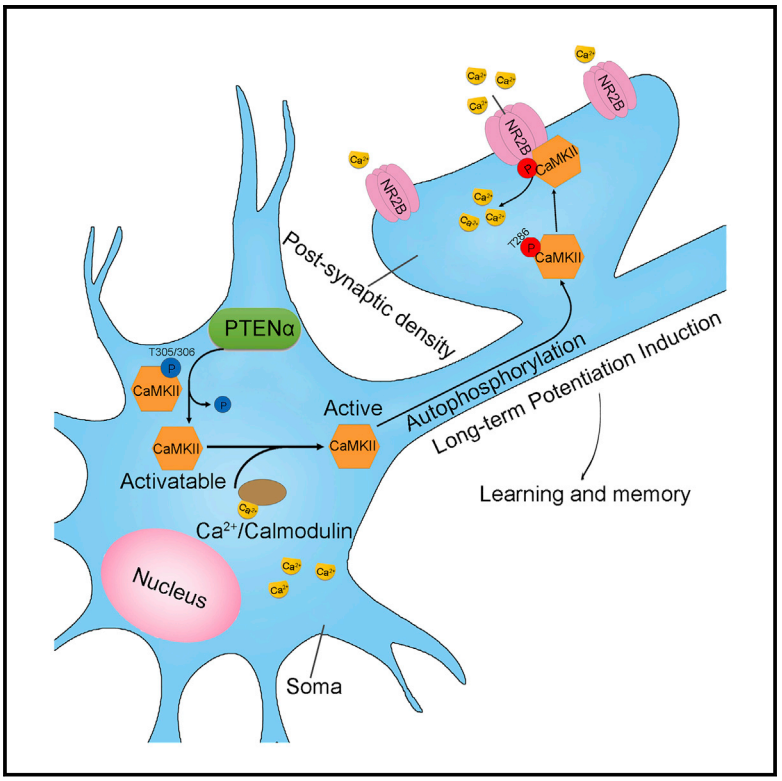

Authors

Pan Wang, Fan Mei, Jiapan Hu, ..., Ruiqi Li, Michael A. McNutt, Yuxin Yin

Correspondence

yinyuxin@hsc.pku.edu.cn

In Brief

Wang et al. define a specific function of PTENα in learning and memory. PTENα maintains CaMKII in an activatable state that is competent to induce long-term potentiation through dephosphorylation of CaMKII at T305/306. Long-term potentiation, contextual fear memory, and spatial learning are impaired in PTENα-specific-deficient mice.

Highlights

- PTENα dephosphorylates and activates CaMKII to promote interaction of CaMKII and NR2B
- PTENα regulates long-term potentiation, fear-conditioned memory, and spatial learning
- CaMKIIα mutations identified in dementia disrupt PTENα-CaMKII-NR2B signaling

Wang et al., 2017, Cell Reports *19*, 2627–2641
June 20, 2017
http://dx.doi.org/10.1016/j.celrep.2017.05.088

Cell Reports
Article

PTENα Modulates CaMKII Signaling and Controls Contextual Fear Memory and Spatial Learning

Pan Wang,[1,2] Fan Mei,[1,2] Jiapan Hu,[1] Minglu Zhu,[1] Hailong Qi,[1] Xi Chen,[1] Ruiqi Li,[1] Michael A. McNutt,[1] and Yuxin Yin[1,3,*]
[1]Institute of Systems Biomedicine, Department of Pathology, School of Basic Medical Sciences, Beijing Key Laboratory of Tumor Systems Biology, Peking-Tsinghua Center for Life Science, Peking University Health Science Center, Beijing 100191, China
[2]These authors contributed equally
[3]Lead Contact
*Correspondence: yinyuxin@hsc.pku.edu.cn
http://dx.doi.org/10.1016/j.celrep.2017.05.088

SUMMARY

PTEN (phosphatase and tensin homology deleted on chromosome 10) has multiple functions, and recent studies have shown that the PTEN family has isoforms. The roles of these PTEN family members in biologic activities warrant specific evaluation. Here, we show that PTENα maintains CaMKII in a state that is competent to induce long-term potentiation (LTP) with resultant regulation of contextual fear memory and spatial learning. PTENα binds to CaMKII with its distinctive N terminus and resets CaMKII to an activatable state by dephosphorylating it at sites T305/306. Loss of PTENα impedes the interaction of CaMKII and NR2B, leading to defects in hippocampal LTP, fear-conditioned memory, and spatial learning. Restoration of PTENα in the hippocampus of PTENα-deficient mice rescues learning deficits through regulation of CaMKII. CaMKII mutations in dementia patients inhibit CaMKII activity and result in disruption of PTENα-CaMKII-NR2B signaling. We propose that CaMKII is a target of PTENα phosphatase and that PTENα is an essential element in the molecular regulation of neural activity.

INTRODUCTION

Long-term potentiation (LTP) of synaptic transmission is a key cellular mechanism underlying different forms of learning and memory (Lee and Silva, 2009; Martin et al., 2000). LTP can be induced in different regions of the brain and requires calcium (Ca^{2+}) influx through N-methyl-D-aspartate receptors (NMDARs) and subsequent activation of Ca2+/calmodulin-dependent kinase protein II (CaMKII) (Kerchner and Nicoll, 2008; Kessels and Malinow, 2009; Malenka and Bear, 2004; Martin et al., 2000). Ca^{2+} influx stimulates not only CaMKII activity, but also stimulates binding of CaMKII to the NMDARs (Bayer et al., 2006; Leonard et al., 1999; Strack and Colbran, 1998) and CaMKII accumulation in the postsynaptic densities (PSD) (Bayer et al., 2006; Shen and Meyer, 1999). NMDARs consist of two GluN1 (NR1) and two GluN2 (NR2A and NR2B) subunits. Activated CaMKII can bind to NR1, NR2A, and NR2B, but its interaction with NR2B is strongest (Gardoni et al., 2001; Leonard et al., 2002; Strack et al., 2000). The major CaMKII binding site on NR2B resides near S1303, and mutation of the primary binding site is sufficient to reduce association of CaMKII with the NMDAR complex and limit maintenance of LTP (Halt et al., 2012), demonstrating that the interaction of CaMKII and NR2B is critical for LTP (Coultrap and Bayer, 2012).

CaMKII is a large holoenzyme consisting of 12 subunits. There are two principal types of CaMKII isoforms in the brain, including CaMKIIα and CaMKIIβ. Once activated by Ca^{2+}/CaM binding, this kinase can be autophosphorylated at threonine 286 (T286 on CaMKIIα and T287 on CaMKIIβ), which leads to persistent CaMKII activation, even after the concentration of Ca^{2+} falls to baseline levels (Buard et al., 2010; Erickson et al., 2008; Hudmon and Schulman, 2002a). Dissociation of Ca^{2+}/CaM from T286-phosphorylated CaMKII triggers threonine 305/306 (T305/306) autophosphorylation (Colbran, 1993), resulting in triple-phosphorylated CaMKII, which is autonomously active, but not competent to be further stimulated (Coultrap et al., 2010). T305/306 residues are located within the Ca^{2+}/CaM region of the regulatory domain, and phosphorylation of these two sites inhibits Ca^{2+}/CaM-binding (Rellos et al., 2010). Dephosphorylation of T305/306 residues therefore enables Ca^{2+}/CaM binding to activate CaMKII. Moreover, a previous study has shown that T305/306 phosphorylation directly affects the interaction of CaMKII and NR2B (Barcomb et al., 2014). These studies indicate that the inhibitory phosphorylation of CaMKII at T305/306 has a critical modulatory role in CaMKII activity, synaptic plasticity, and learning. However, the phosphatase, which acts on the T305/306 residues, has heretofore not been identified.

PTENα is an isoform of phosphatase and tensin homology deleted on chromosome 10 (PTEN) that is translated through a non-canonical CUG-initiated mechanism. It contains a 403-amino acid canonical PTEN sequence and an evolutionarily conserved 173-amino acid N terminus (Hopkins et al., 2013; Liang et al., 2014). Hopkins et al. (2013) reported that there is a secretion signal and a re-entry sequence located in the N terminus of PTENα that enables the protein to be secreted from one cell to an adjacent cell, and PTENα contributes to suppression

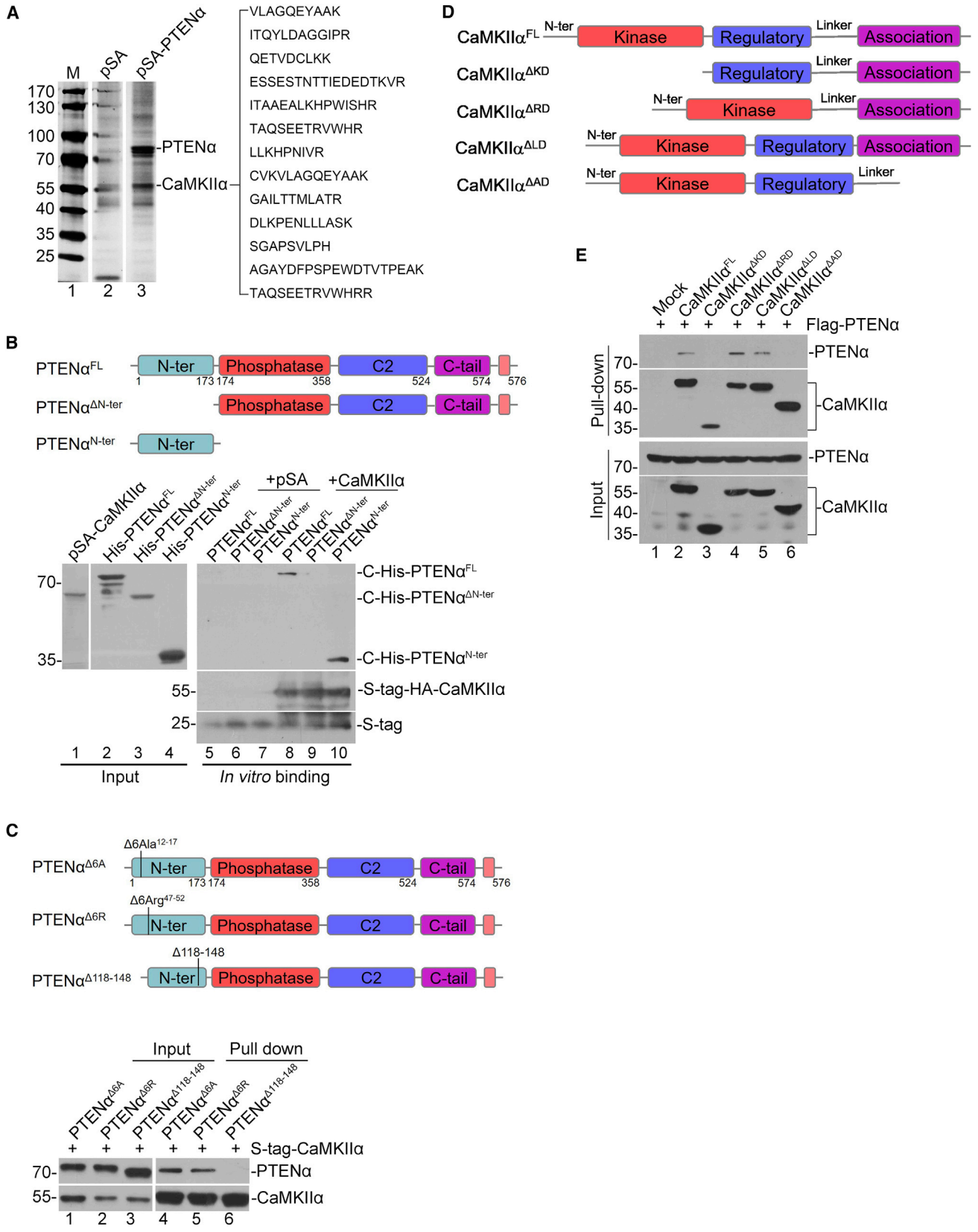

(legend on next page)

of cancer by acting as an antagonist of the phosphatidylinositol 3-kinase (PI3K) pathway. Our laboratory discovered PTENα also localizes in mitochondria and interacts with canonical PTEN to increase PINK1 expression and promote energy production (Liang et al., 2014). These studies all show that the extended N terminus of PTENα confers specific functions, which are different from PTEN, raising the possibility that there may be additional distinct undiscovered PTENα functions.

"PTEN knockout" mouse models exhibit severe neural dysfunction, including anxiety, "autism-like" behavioral deficits (Lugo et al., 2014), spontaneous seizures, ataxia, macrocephaly, and Lhermitte-Duclos disease (Backman et al., 2001; Kwon et al., 2001). However, both PTEN and PTENα were deleted in these previous PTEN knockout mouse models and the observed phenotypes, in fact, resulted from the loss of both PTEN and PTENα. In this study, we generated a specific PTENα knockout mouse model that maintains PTEN expression, allowing specific evaluation of PTENα function in vivo. Our study illustrates the mechanism by which PTENα regulates learning and memory through control of CaMKIIα phosphorylation.

RESULTS

PTENα Primarily Resides in Neurons and Is Involved in Neural Regulation

We examined the tissue distribution of PTENα in mice with an anti-PTEN antibody that recognizes both PTEN and PTENα and found that PTENα is highly expressed in different regions of the mouse brain (Figure S1A). To further investigate PTENα expression and function, we generated a PTENα-specific monoclonal antibody against the intact N terminus region of PTENα. Using this antibody, we observed PTENα resides primarily in neurons rather than in the glia (Figures S1B–S1D), indicating that PTENα may be involved in neuronal activities.

To probe for PTENα substrates in the brain, we purified exogenous PTENα with S-protein beads, followed by incubation with lysates from mouse brain, and the precipitates were analyzed by mass spectrometry. A long list of PTENα-interacting candidates was identified (Table S1). Kyoto Encyclopedia of Genes and Genomes (KEGG) pathway enrichment analysis with these molecules showed that they are involved in multiple neural pathways, including LTP and the glutamatergic synapse pathway (Figure S2A). Networking analysis with the STRING database was used to evaluate the importance of PTENα-interacting proteins in reported cellular process regulation, and there were 30 proteins located in important nodes (Figure S2B), including PTEN as previously reported (Liang et al., 2014).

As PTENα is a phosphatase protein (Hopkins et al., 2013), we generated a proteomic peptide library and subsequently performed in vitro phosphatase assays together with mass spectrometry to evaluate the phosphatase activity of PTENα (Figure S3A). As shown in Table S2, phosphorylation levels of PTENα-interacting candidates (23 out of 37 proteins) involved in neural regulation were decreased by PTENα, raising the possibility that PTENα regulates these proteins. These bioinformatics data reflect the importance and complexity of PTENα in neural regulation.

PTENα Binds Directly to CaMKIIα with Its Distinctive N terminus

CaMKIIα, which localizes in neurons, was found to be one of the PTENα-interacting candidates (Figures S2A and S2B), and a total of 13 CaMKIIα peptides were identified in the PTENα precipitation (Figure 1A). Reciprocal immunoprecipitation performed in lysates from HEK293T cells co-transfected with PTENα and CaMKIIα confirmed PTENα interacts with CaMKIIα (Figures S3B and S3C). Using immunofluorescence in primary neurons and transfected SHSY5Y cells, we observed co-localization of both endogenous and exogenous PTENα and CaMKIIα in cytoplasm (Figure S3D), and this spatial co-location serves as a foundation for the interaction of PTENα and CaMKIIα.

The PTENα sequence 174–576 amino acid (aa) is identical to PTEN, which raised a question as to whether CaMKIIα binds PTENα or PTEN. In vitro binding experiments with purified full-length PTENα (PTENα^{FL}) and PTENα truncations showed that CaMKIIα binds to PTENα^{FL} and PTENα$^{N\text{-}ter}$ (N-terminus) (Figure 1B, lanes 8 and 10 versus lane 9). More specifically, PTENα$^{\Delta 118–148}$ loses the ability to bind to CaMKIIα (Figure 1C, lane 6 versus lanes 4 and 5), demonstrating that the 118–148 aa fragment of PTENα is required for CaMKIIα and PTENα interaction. In reciprocal experiments, S-tag pull down performed with HEK293T cell lysates showed kinase domain deleted CaMKIIα$^{\Delta KD}$ and association domain deleted CaMKIIα$^{\Delta AD}$ lose the ability to interact with PTENα (Figures 1D and 1E, lanes 3 and 6 versus lane 2), implying that both the kinase domain and the association domain of CaMKIIα are necessary for PTENα binding. Based on the crystal structure of CaMKII in the basal state, the regulatory domain blocks the substrate binding site of the kinase domain (Chao et al., 2011; Krapivinsky et al., 2004; Rellos et al., 2010), indicating that autoinhibition prevents

Figure 1. PTENα Directly Interacts with CaMKIIα through Its Distinctive N terminus

(A) Silver staining and mass spectrometry (MS) analysis of PTENα-associated proteins after precipitation (with S-protein beads) from cortical lysates with S-tagged PTENα purified from HEK293T transfected cells. There were 13 matched peptide sequences that corresponded to CaMKIIα.

(B) Upper panel, schematic structure of recombinant His-PTENα^{FL} (aa 1–576), His-PTENα$^{\Delta N\text{-}ter}$ (aa 174–576, identical to PTEN), and His-PTENα$^{N\text{-}ter}$ (aa 1–173). The lower panel shows recombinant proteins that were incubated with S-tagged CaMKIIα purified from HEK293T transfected cells and lysates precipitated with S-protein beads that were immunoblotted with His or HA antibody.

(C) Upper panel, schematic illustration of PTENα deletions. The lower panel shows an interaction of PTENα deletions with S-tagged CaMKIIα in HEK293T cells. Lysates precipitated with S-protein beads were immunoblotted with FLAG or HA antibody.

(D) Schematic representation of a series of CaMKIIα^{FL}, CaMKIIα deletion, and truncation mutant vectors. Plasmids were cloned into a pSA-N vector. CaMKIIα$^{\Delta KD}$ (kinase domain deleted), CaMKIIα$^{\Delta RD}$ (regulatory domain deleted), CaMKIIα$^{\Delta LD}$ (linker deleted), CaMKIIα$^{\Delta AD}$ (association domain deleted).

(E) HEK293T cells were co-transfected with S-tagged CaMKIIα^{FL}, CaMKIIα$^{\Delta KD}$, CaMKIIα$^{\Delta RD}$, CaMKIIα$^{\Delta LD}$, CaMKIIα$^{\Delta AD}$, and FLAG-PTENα, and cell lysates were pulled down with S-protein beads and subjected to immunoblot with FLAG or HA antibody.

See also Figures S1–S3 and Table S1.

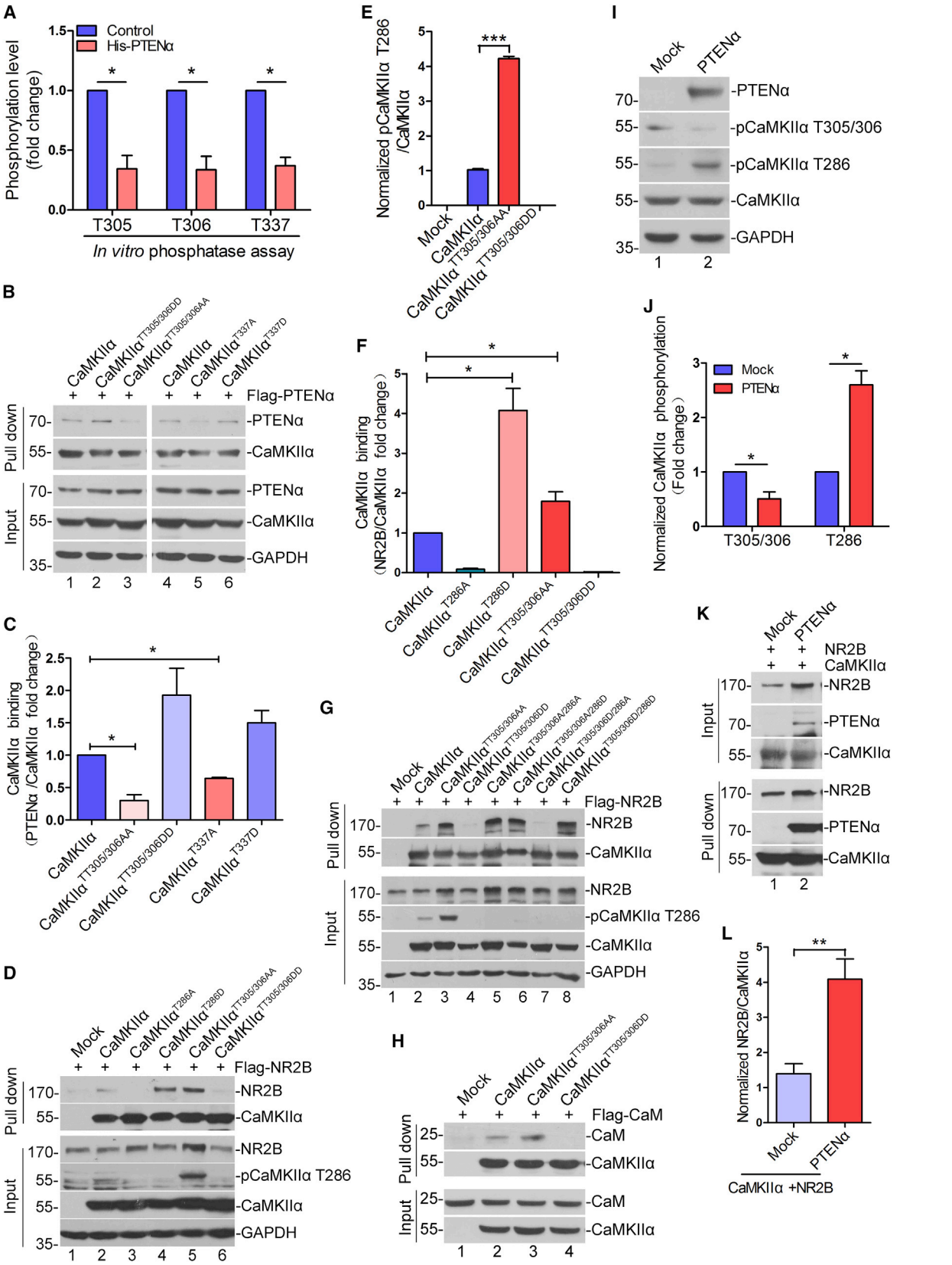

(legend on next page)

CaMKII protein interactions that occur at the S-site or at the T-site (Coultrap and Bayer, 2012). Moreover, it is generally thought that the holoenzyme structure is required for some CaMKII functions, such as T286 phosphorylation and NR2B binding (Coultrap and Bayer, 2012). CaMKIIα$^{\Delta AD}$ is unable to form a CaMKII holoenzyme and interact with PTENα, indicating that the CaMKII holoenzyme structure is required for its binding with PTENα.

PTENα Dephosphorylates CaMKII T305/306 and T337 Sites to Facilitate CaMKII Activity and NR2B Binding

Phosphorylation of CaMKII provides important mechanisms for regulation of kinase activity and protein interactions (Coultrap and Bayer, 2012). We found CaMKIIα phosphorylation was modified by PTENα (Table S2), leading us to evaluate CaMKIIα dephosphorylation by PTENα. Using an in vitro phosphatase assay (Figures S4A and S4B), followed by mass spectrometry, we observed that incubation of CaMKIIα with PTENα results in dephosphorylation of multiple CaMKIIα residues and three residues in particular attracted our attention (Figures 2A and S4C). Two of these three residues, T305 and T306, have been reported to influence CaMKII activity (Colbran, 1993; Elgersma et al., 2002). No function has been reported for the third of these residues T337 (Huttlin et al., 2010). To support these findings, we generated threonine (T) to alanine (A) or aspartic acid (D) point mutants at each site and found that binding of PTENα to two CaMKIIα mutants (TT305/306AA and T337A) was obviously reduced (Figures 2B, lanes 3 and 5 versus lanes 1 and 4, and 2C), demonstrating that phosphorylation of these residues is critical for the direct interaction of CaMKIIα and PTENα.

T305/306 phosphorylation prevents Ca^{2+}/CaM binding and subsequent autophosphorylation at T286 (Colbran, 1993; Lu et al., 2003). We expressed CaMKIIα TT305/306AA (non-phosphorylation state mimic) and TT305/306DD (phosphorylation state mimic) mutants in HEK293T cells to evaluate CaMKIIα T286 phosphorylation levels. When T was mutated to A at sites 305/306, T286 phosphorylation was dramatically increased (Figures 2D, lane 5 versus lane 2, and 2E). In contrast, when T was mutated to D, phosphorylation at T286 was obviously blocked (Figures 2D, lane 6 versus lane 2, and 2E).

We next analyzed the effect of CaMKIIα phosphorylation on its binding with NR2B in HEK293T cells. Consistent with previous reports (Halt et al., 2012; Sanhueza et al., 2011), there was a strong interaction between the CaMKIIα T286D (phosphorylation state mimic) mutant and NR2B (Figures 2D, lane 4 versus lane 2, and 2F), while CaMKIIα T286A (non-phosphorylation state mimic) showed decreased NR2B binding as compared with wild-type CaMKIIα (Figures 2D, lane 3 versus lane 2, and 2F), validating the reliability of this assay. Using the same assay, we evaluated the effects of T305/306 phosphorylation on the interaction of CaMKIIα and NR2B. As expected, the CaMKIIα TT305/306AA mutant interacted strongly with NR2B (Figures 2D, lane 5 versus lane 2, and 2F), while the CaMKIIα TT305/306DD mutant showed no association with NR2B (Figures 2D, lane 6 versus lane 2, and 2F).

To address the issue of crosstalk between T286 and T305/306 phosphorylation in regulation of CaMKII/NR2B binding, triple mutants of CaMKIIα were used. When the phosphorylation effect of CaMKIIα T305/306 was mimicked by TT305/306DD, interaction with NR2B depended on T286 phosphorylation (Figure 2G, lanes 7 and 8 versus lane 2). When the dephosphorylation effect of CaMKIIα T305/306 was mimicked by TT305/306AA, physical association of CaMKIIα and NR2B occurred regardless of the phosphorylation status of T286 (Figure 2G, lanes 5 and 6 versus lane 2). These results are consistent with CaMKIIα T305/306 phosphorylation directly affecting NR2B binding (Barcomb et al., 2014). Moreover, we observed stronger interaction of CaMKIIα TT305/306AA with CaM as compared to CaMKIIα (Figure 2H, lane 3 versus lane 2). Our data thus reveal dephosphorylation of CaMKIIα T305/306 promotes NR2B binding by either T286 phosphorylation or Ca^{2+}/CaM binding.

Mouse T337, which is equivalent to human T348, is located in the association domain (Figure S5A), which indicates T337 phosphorylation may coordinate CaMKII function. We found that

Figure 2. PTENα Dephosphorylates CaMKIIα at T305/306 and T337 to Facilitate T286 Phosphorylation and CaMKIIα-NR2B Interaction

(A) Quantitative analysis of CaMKIIα phosphorylation in in vitro phosphatase assays. Exogenous CaMKIIα purified from HEK293T cells was used as substrate and PTENα purified from SF9 cells was used as phosphatase. The phosphorylation status of T305/306 and T337 was significantly reduced (n = 3 replicates).

(B) Immunoassay of HEK293T cells transfected with FLAG-PTENα and S-tagged CaMKIIα or CaMKIIα mutants. Lysates precipitated with S-protein beads were analyzed by immunoblot analysis with FLAG or HA antibody.

(C) Quantitative analyses of CaMKIIα mutants interact with PTENα (n = 3 replicates).

(D) HEK293T cells were co-transfected with S-tagged CaMKIIα, CaMKIIα$^{TT305/306AA}$, CaMKIIα$^{TT305/306DD}$, CaMKIIα^{T286A}, or CaMKIIα^{T286D} with FLAG-NR2B. Cell lysates were pulled down with S-protein beads and analyzed by immunoblot with NR2B and pCaMKIIα^{T286} antibodies.

(E) Quantitative analyses of CaMKIIα T286 phosphorylation in HEK293T cells transfected with TT305/306AA and TT305/306DD mutants with p-CaMKIIα^{T286} antibody (n = 3 replicates).

(F) Quantitative analyses of CaMKIIα mutants-associated NR2B (n = 5 replicates).

(G) HEK293T cells were co-transfected to express FLAG-tagged NR2B with S-tagged CaMKIIα, CaMKIIα$^{TT305/306AA}$, CaMKIIα$^{TT305/306DD}$, CaMKIIα$^{T305/306A/286A}$, CaMKIIα$^{T305/306A/286D}$, CaMKIIα$^{T305/306D/286A}$, or CaMKIIα$^{T305/306D/286D}$. Cell lysates were then precipitated with S-protein beads and subjected to immunoblot.

(H) HEK293T cells were co-transfected with S-tagged CaMKIIα, CaMKIIα$^{TT305/306AA}$, CaMKIIα$^{TT305/306DD}$, with FLAG-CaM. Cell lysates were pulled down with S-protein beads and analyzed by immunoblot with anti-FLAG and anti-HA antibodies.

(I) Immunoblot analysis of CaMKIIα T305/306 and T286 phosphorylation in SHSY5Y cells transfected with PTENα.

(J) Quantitative analysis of CaMKIIα T305/306 and T286 phosphorylation in SHSY5Y cells transfected with PTENα (n = 3 replicates).

(K and L) Western blot and quantitative analysis showed PTENα promotes the interaction of CaMKIIα and NR2B.

(K) HEK293T cells were transfected with FLAG-PTENα^{FL} or mock with FLAG-NR2B and S-tagged CaMKIIα. Cell lysates were pulled down with S-protein beads and subjected to immunoblot with anti-NR2B antibody.

(L) Quantitative analysis of CaMKIIα-associated NR2B (n = 5 replicates).

*p < 0.05, **p < 0.01, and ***p < 0.001. The data represent mean ± SEM. See also Figures S4 and S5 and Table S2.

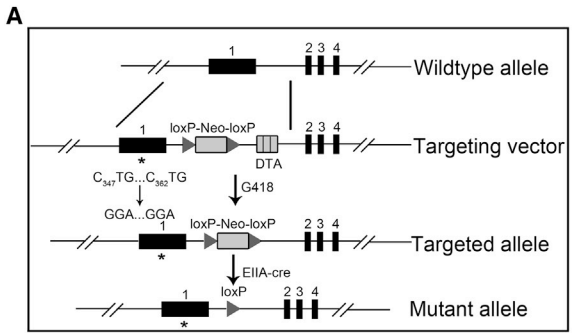

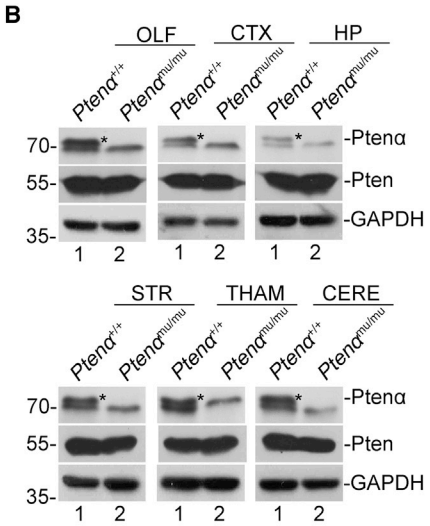

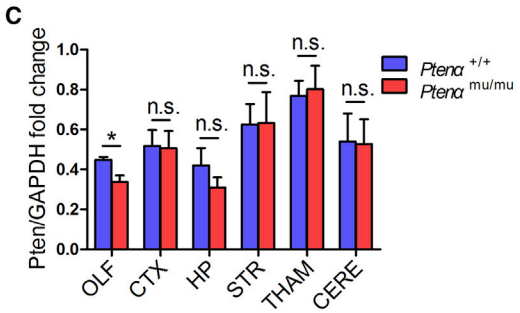

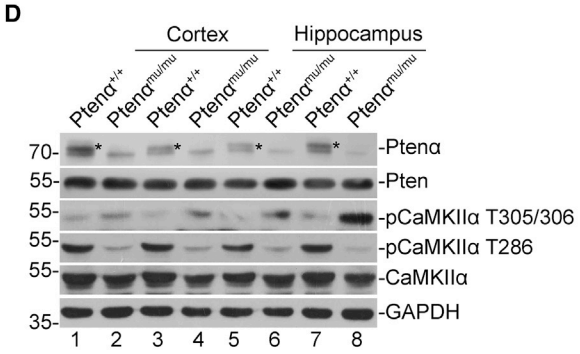

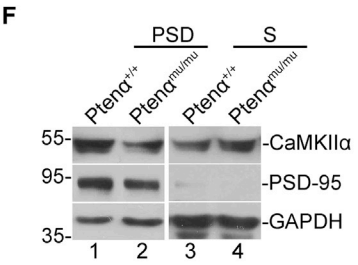

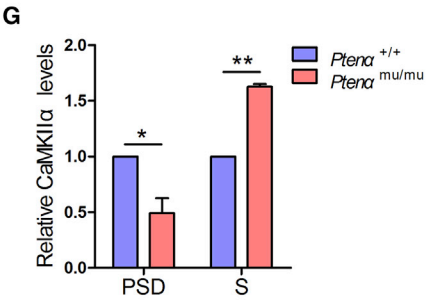

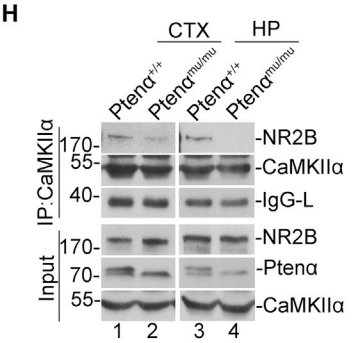

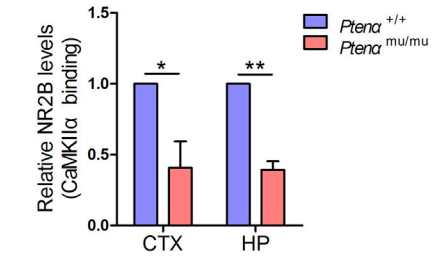

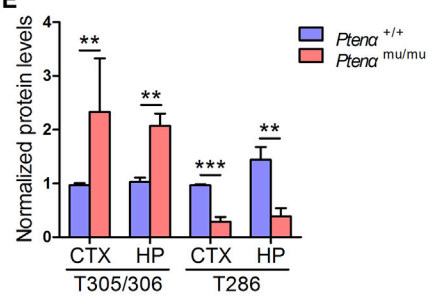

(legend on next page)

CaMKIIα T337 phosphorylation has no effect on T286 phosphorylation (data not shown). However, the CaMKIIα T337D mutant showed decreased NR2B binding as compared with the wild-type protein (Figures S5A, lane 7 versus lane 6, and S5B). Moreover, we found extremely weak association of CaMKIIα T337D and CaM (Figure S5C, lanes 5 and 4 versus lane 2), implying that T337 phosphorylation makes CaMKII less accessible for CaM binding. These results indicate T337 phosphorylation prevents CaMKIIα-NR2B interaction by blocking Ca^{2+}/CaM binding.

Our observations demonstrate phosphorylation drives CaMKII activity, and the T286 phosphorylation level and CaMKIIα-NR2B interaction can be used as specific indicators of CaMKII activity. Of note, overexpression of PTENα in SHSY5Y cells repressed endogenous CaMKIIα T305/306 phosphorylation, leading to up-regulation of T286 phosphorylation (Figures 2I and 2J). Consistent with these findings, we observed CaMKIIα co-expressed with PTENα showed increased association with NR2B (Figures 2K and 2L). These data indicate that PTENα increases CaMKII activity by dephosphorylation of T305/306 and T337.

PTENα Loss In Vivo Impedes CaMKII PSD Localization and CaMKII-NR2B Interaction

After establishing that PTENα alters CaMKII activity in vitro, we investigated the impact of PTENα loss on CaMKII signaling in vivo. Mutation of human PTENα CTG513 to GGA completely abolished PTENα expression without affecting PTEN (Liang et al., 2014). We thus substituted the two CTG codons of mouse *Pten*α (CTG347 … CTG362, which are equivalent to *Homo sapiens* CTG513) with GGA (Figure 3A). Sequencing confirmed replacement of CTG347 and CTG362 by GGA in both alleles in the genome of homozygous PTENα knockout mice (designated *Pten*$\alpha^{mu/mu}$) (Figure S5D). Mice used for subsequent experiments were genotyped by PCR with specific primers, in which the mutant allele was longer than the wild-type allele (Figure S5E). Western blot was used to evaluate PTENα expression in the PTENα wild-type (*Pten*$\alpha^{+/+}$) and *Pten*$\alpha^{mu/mu}$ mouse brain and showed expression was completely abolished in various regions of the *Pten*$\alpha^{mu/mu}$ brain, while canonical PTEN remained unaffected except for the PTEN level in the olfactory bulb, which was slightly reduced (Figures 3B and 3C), validating the specificity of this mouse model.

In keeping with our previous data from cell experiments, PTENα ablation resulted in increased CaMKIIα T305/306 phosphorylation and decreased T286 phosphorylation (Figures 3D and 3E). Mass spectrometry showed T337 phosphorylation (T9 site in the sequence ESSESTNTTEDEDTK is equivalent to the CaMKIIα T337 site) was increased in *Pten*$\alpha^{mu/mu}$ mice as well (Figure S5F, phosphorylation level is represented by "Area"). CaMKII phosphorylation has been consistently linked to Ca^{2+} stimulation and CaM binding (Lisman et al., 2002). However, we observed Ca^{2+} fluxes behaved similarly in *Pten*$\alpha^{+/+}$ and *Pten*$\alpha^{mu/mu}$ primary neurons with KCl stimulation (Figure S5G), and CaM showed identical expression in *Pten*$\alpha^{+/+}$ and *Pten*$\alpha^{mu/mu}$ mice (Figures S5H and S5I), indicating that alterations of CaMKIIα phosphorylation, which occur in *Pten*$\alpha^{mu/mu}$ mice, are direct results of PTENα deletion.

The binding of CaMKII to PSD and NMDA receptors can be regulated by its autophosphorylation at T286 and T305/306 (O'Leary et al., 2011). We therefore evaluated the binding efficiency of CaMKII with PSD in *Pten*$\alpha^{mu/mu}$ mice using PSD fractionation, followed by immunoblot analysis. PSD-associated CaMKIIα protein was reduced by ~35% in *Pten*$\alpha^{mu/mu}$ mice as compared to *Pten*$\alpha^{+/+}$ mice (Figures 3F and 3G). To assess the binding of CaMKII to NMDA receptors, we analyzed the interaction of CaMKIIα and NR2B in *Pten*$\alpha^{+/+}$ and *Pten*$\alpha^{mu/mu}$ mice. Co-immunoprecipitation of CaMKIIα in lysates from *Pten*$\alpha^{+/+}$ and *Pten*$\alpha^{mu/mu}$ mice showed that interaction of NR2B and CaMKIIα is significantly attenuated in *Pten*$\alpha^{mu/mu}$ mice (Figures 3H and 3I). These data indicate PTENα regulates the localization of CaMKII in PSD and interaction with NMDARs through dephosphorylation of CaMKII in vivo.

CaMKII-Mediated LTP Is Impaired in PTENα-Deficient Mice

CaMKII is a component of the crucial cellular mechanism underlying LTP (Lisman et al., 2002), and this raised the possibility PTENα may regulate synaptic plasticity. We first performed field recordings of excitatory postsynaptic potentials (fEPSPs) in acute hippocampal slices. The input-output curves for fEPSPs showed no differences in the *Pten*$\alpha^{mu/mu}$ and wild-type phenotypes (Figure 4A), suggesting that basal excitatory transmission is normal in *Pten*$\alpha^{mu/mu}$ mice. Hippocampal LTP was induced in the Schaffer collateral pathway using a high-frequency train (100 Hz for 1 s) and was found to be significantly reduced in *Pten*$\alpha^{mu/mu}$ mice (Figures 4B and 4C). Paired-pulse facilitation was intact over a range of interpulse intervals (Figure 4D), indicating that there were no defects in presynaptic transmitter release in *Pten*$\alpha^{mu/mu}$ mice. To examine the mechanism

Figure 3. Dysregulation of CaMKII Signaling in *Pten*$\alpha^{mu/mu}$ Mice

(A) Schematic representation of strategy for generation of *Pten*α mutant mice. The CTG ($CTG^{347;362}$) translation start codons of *Mus musculus Pten*α equivalent to the *Homo sapiens* codon CTG^{513} in exon 1 were replaced with GGA.

(B) Immunoblot showing PTENα and PTEN expression in *Pten*$\alpha^{+/+}$ and *Pten*$\alpha^{mu/mu}$ mice. Olfactory bulb (OLF), cortex (CTX), hippocampus (HP), striatum (STR), thalamus (THAM), and cerebellum (CERE) are shown as indicated. "*"-labeled upper band refers to PTENα.

(C) Quantification of PTEN expression in lysates from *Pten*$\alpha^{+/+}$ and *Pten*$\alpha^{mu/mu}$ mice (PTEN levels were normalized with GAPDH. n = 5 per genotype).

(D) Western blot analysis of CaMKIIα expression and phosphorylation in cortical and hippocampal lysates from *Pten*$\alpha^{mu/mu}$ (n = 2) and *Pten*$\alpha^{+/+}$ mice (n = 2). *-labeled upper band refers to PTENα.

(E) Quantitative analysis of CaMKIIα T305/306 and T286 phosphorylation in cortical and hippocampal lysates from *Pten*$\alpha^{mu/mu}$ (n = 6) and *Pten*$\alpha^{+/+}$ mice (n = 6).

(F and G) Western blot analysis and quantification of PSD-enriched fractions isolated from *Pten*$\alpha^{+/+}$ and *Pten*$\alpha^{mu/mu}$ mice. (F) Representative blotting showing PSD-95 and CaMKIIα. (G) Quantitative analysis of PSD-associated CaMKIIα. Levels of CaMKIIα were normalized with PSD-95 or GAPDH (n = 3 replicates).

(H and I) Immunoblots (H) and quantitative analysis (I) of co-precipitation of NR2B in cortical and hippocampal lysates from *Pten*$\alpha^{+/+}$ and *Pten*$\alpha^{mu/mu}$ mice with anti-CaMKIIα antibody, NR2B levels were normalized with CaMKIIα (n = 3 replicates).

*p < 0.05, **p < 0.01, and ***p < 0.001. The data represent mean ± SEM. See also Figure S5.

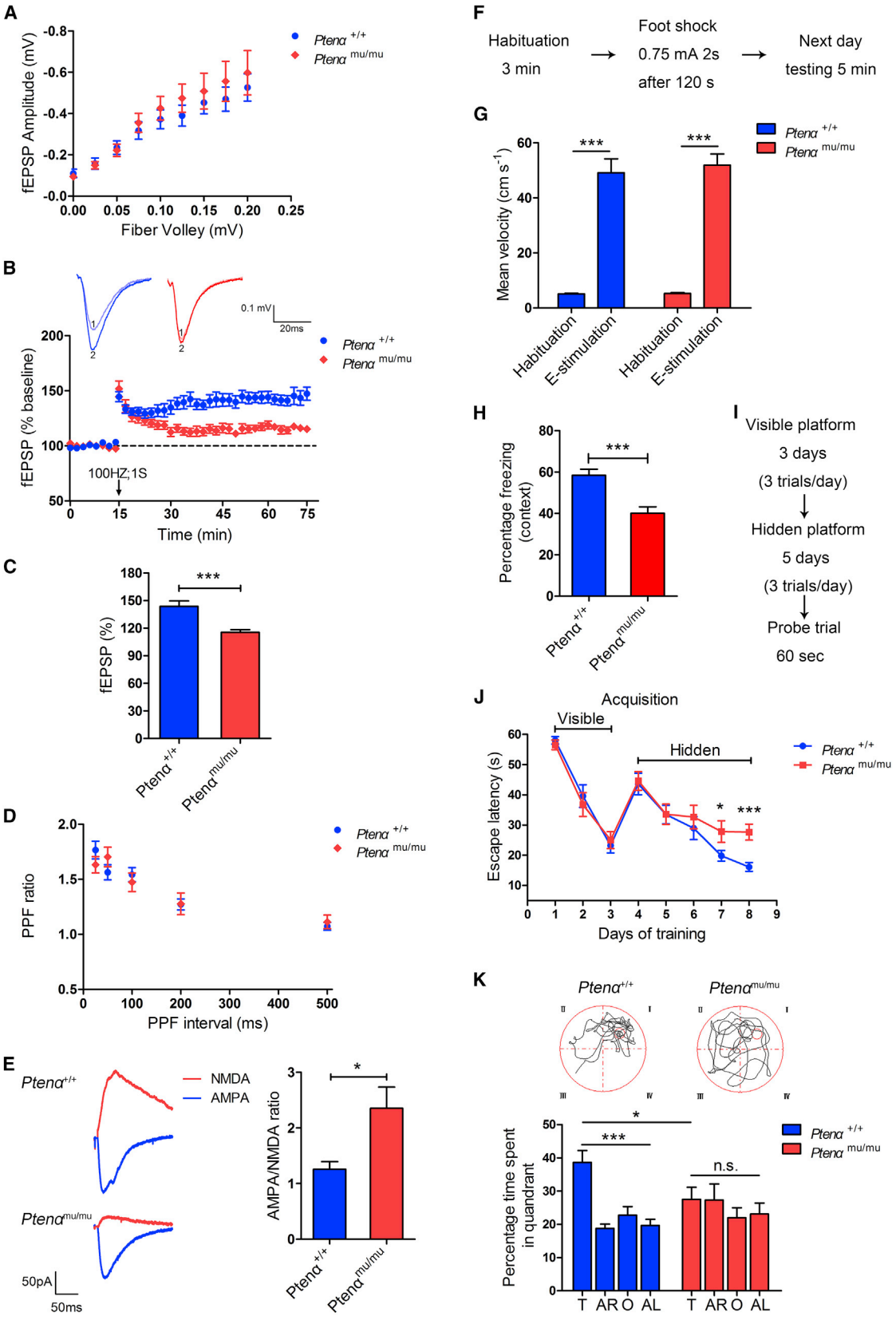

(legend on next page)

underlying LTP impairment, we applied a whole-cell patch and found the α-amino-3-hydroxy-5-methyl-4-isoxazole-propionic acid (AMPA)/NMDA current ratio was significantly increased in *Pten*α$^{mu/mu}$ mice (Figure 4E). These results demonstrate PTENα is required for LTP.

The PI3K/AKT pathway is a common target of PTEN and PTENα (Backman et al., 2001; Hopkins et al., 2013) and is involved in neural function regulation (Backman et al., 2001). Thus, it is possible that PTENα regulates LTP in concert with this pathway. However, examination of PI3K signaling by analysis of the status of AKT phosphorylation and mammalian target of rapamycin (mTOR) phosphorylation showed no significant change in the PI3K/AKT pathway in *Pten*α$^{mu/mu}$ mice (Figures S6A and S6B). These findings indicate the LTP deficits in *Pten*α$^{mu/mu}$ mice are likely due to CaMKII dysfunction.

Contextual Fear Memory and Spatial Learning Are Impaired in PTENα-Deficient Mice

It was previously reported PTEN brain knockout mice exhibit severe developmental deficits and have a shortened lifespan (Backman et al., 2001). However, *Pten*α$^{mu/mu}$ mice showed normal fertility, birth rate, and body weight as compared with *Pten*α$^{+/+}$ littermates (Figures S6C and S6D). Moreover, the hippocampus and cortex in *Pten*α$^{mu/mu}$ mice were morphologically normal (Figure S6E), and there were no developmental defects in these mice.

CaMKII plays a critical role in fear-conditioned memory and spatial learning (Elgersma et al., 2002; Giese et al., 1998; Silva et al., 1992), raising the possibility that PTENα participates in learning and memory regulation. We therefore performed contextual fear condition memory tests (Elgersma et al., 2002), in which mice were given a mild aversive foot shock (Figure 4F). *Pten*α$^{+/+}$ and *Pten*α$^{mu/mu}$ mice both displayed a similar aversive reaction to foot shock (Figure 4G). However, recall memory of the conditioning chamber measured by freezing behavior was impaired in *Pten*α$^{mu/mu}$ mice, as compared with control cohorts (Figure 4H).

Morris water maze (MWM) trials were performed to evaluate spatial learning (Figure 4I). *Pten*α$^{mu/mu}$ mice behaved normally in visual training sessions. However, in the hidden training sessions on day 7 and day 8, acquisition of spatial learning in *Pten*α$^{+/+}$ control mice, as reflected in reduced latency in reaching the hidden platform, was not observed in *Pten*α$^{mu/mu}$ mice (Figure 4J). To assess reference memory, we performed a probe trial 24 hr after the final training session, during which the platform was removed. As expected, *Pten*α$^{mu/mu}$ mice had diminished memory recall, as indicated by reduced time spent in the target quadrant (Figure 4K). There was no obvious difference in swimming speed in *Pten*α$^{+/+}$ and *Pten*α$^{mu/mu}$ cohorts during the probe trial (Figure S6F).

We performed additional behavioral tasks to test for locomotor activity (Figures S6G–S6I) and emotional problems (Figures S6J–S6N) and found no differences in *Pten*α$^{+/+}$ and *Pten*α$^{mu/mu}$ mice, suggesting that the impaired performance in *Pten*α$^{mu/mu}$ mice was not the result of locomotor activity or anxiety.

Restoring PTENα Expression in the Hippocampus Reverses Spatial Learning Deficits in PTENα-Deficient Mice

In view of the fact PTENα can reset CaMKII to an activatable state in vitro, we reasoned that restoration of PTENα in PTENα-deficient mice might rescue the defects in these mice by regulating CaMKII. Since PTENα expression is relatively low in tissues as compared to PTEN (Figure S1A), we generated a lentivirus containing human PTENα cDNA with a woodchuck hepatitis posttranscriptional regulatory element (WPRE) (Figure 5A). Lenti-PTENα-GFP or Lenti-GFP was injected bilaterally into the hippocampus of 2- to 3-month-old mice (Figure 5B). At 1 week after injection, Lenti-GFP or Lenti-PTENα-GFP was expressed in the dentate gyrus (DG) and CA1 of the hippocampus (Figure 5C). GFP or GFP-PTENα protein represented by GFP expression was equally expressed in the hippocampus of PTENα- or GFP-injected *Pten*α$^{mu/mu}$ mice and GFP-injected *Pten*α$^{+/+}$ mice (Figure 5D). Exogenous expression of PTENα in *Pten*α$^{mu/mu}$ mice led to decrease of T305/306 phosphorylation to the same extent as that in *Pten*α$^{+/+}$ mice and increased T286 phosphorylation to a lesser extent as compared to *Pten*α$^{+/+}$ mice (Figures 5D and 5E). Resultant behavioral changes of

Figure 4. LTP, Fear Condition Memory, and Spatial Learning Are Impaired in *Pten*α$^{mu/mu}$ Mice

(A) Normal basal synaptic transmission. Input-output curves were generated by plotting postsynaptic fEPSP amplitude as a function of presynaptic fiber volley *Pten*α$^{+/+}$: nine slices, three mice; *Pten*α$^{mu/mu}$: seven slices, four mice (two-way ANOVA, p = 0.129).

(B and C) PTENα loss impairs LTP at the Schaffer collateral pathway in acute hippocampal slices. (B) LTP (1 × 100 Hz/1 s) was significantly impaired in *Pten*α$^{mu/mu}$ mice. (C) LTP stabilized at 143.7% ± 5.8% (*Pten*α$^{+/+}$ mice) and at 115.5% ± 2.8% (*Pten*α$^{mu/mu}$ mice) of baseline (t test, at 50–60 min after induction; ***p < 0.001). An example of averaged traces before (1) and after (2) LTP induction are shown (insets). *Pten*α$^{+/+}$: six slices, five mice; *Pten*α$^{mu/mu}$: eight slices, seven mice.

(D) Normal paired-pulse facilitation (PPF). The ratio of the second and first fEPSP slopes was calculated. *Pten*α$^{+/+}$: nine slices, three mice; *Pten*α$^{mu/mu}$: seven slices, three mice, analyzed with two-way ANOVA, p = 0.934.

(E) AMPA receptor-mediated currents were measured at the peak of the currents (−60 mV), NMDA currents were measured 50 ms after onset at a holding potential of 40 mV, in the presence of picrotoxin (80 μM). The left panel shows an example of NMDA and AMPA traces. The right panel shows the AMPA/NMDA current ratio was 1.26 ± 0.14 in *Pten*α$^{+/+}$ mice (seven cells, three mice) and 2.35 ± 0.38 in *Pten*α$^{mu/mu}$ mice (eight cells, four mice) (two-tailed unpaired t test, p = 0.024).

(F) Schematic illustration of contextual fear-conditioned memory process (*Pten*α$^{+/+}$ n = 18, *Pten*α$^{mu/mu}$ n = 17).

(G) Mean velocity (mm s^{-1}) measured during the habituation and E-stimulation phases on the training day for fear-conditioned learning.

(H) Contextual fear conditioning memory scored as percent time spent freezing during a 5 min exposure to the context.

(I–K) Data from the Morris water maze with *Pten*α$^{mu/mu}$ mice and *Pten*α$^{+/+}$ control siblings (*Pten*α$^{+/+}$ n = 18, *Pten*α$^{mu/mu}$ n = 15). (I) Design of Morris water maze. (J) During the learning stage, *Pten*α$^{mu/mu}$ mice spent more time to reach the platform than controls. (K) Upper panel, representative exploration route of *Pten*α$^{+/+}$ and *Pten*α$^{mu/mu}$ mice in the probe trial on day 9; lower panel, percentage time spent in quadrant, *Pten*α$^{mu/mu}$ mice performed significantly worse in the probe trail on day 9. T, targeted quadrant; R, right quadrant; O, opposite quadrant; L, left quadrant. *p < 0.05, **p < 0.01, and ***p < 0.001. The data represent mean ± SEM. See also Figure S6.

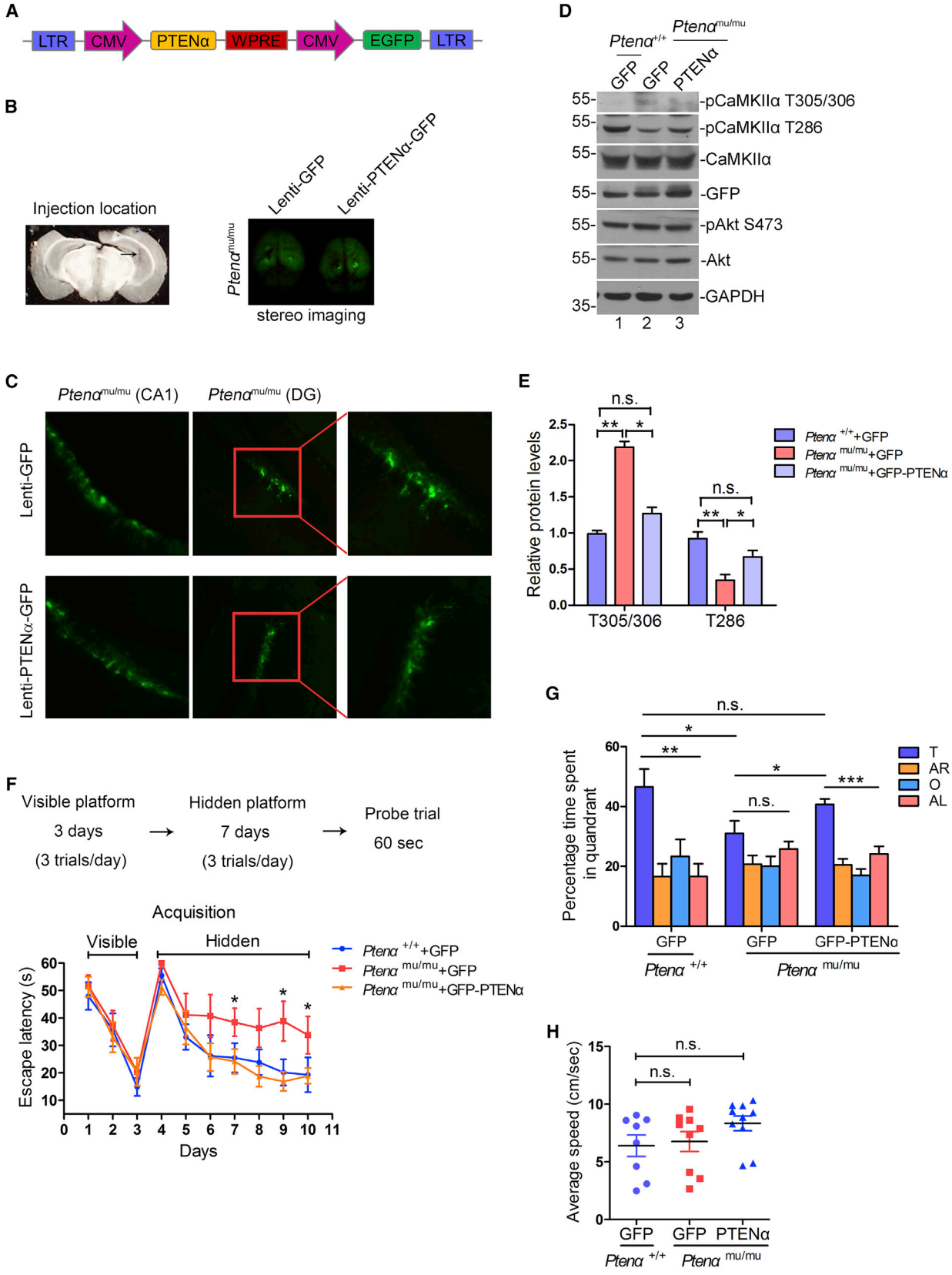

(legend on next page)

injected mice were analyzed with the Morris water maze. As compared with GFP-injected *Pten*$\alpha^{mu/mu}$ controls, spatial learning defects were largely rescued by PTENα re-expression in *Pten*$\alpha^{mu/mu}$ mice (Figures 5F–5H). These results argue introduction of PTENα into the hippocampus is sufficient to repair the spatial learning deficits through regulation of CaMKII.

CaMKIIα Mutations Identified in Dementia Patients Disrupt PTENα-CaMKIIα-NR2B Signaling

The PTENα-CaMKIIα-NR2B axis plays an essential role in learning and memory as demonstrated by observations in this study, raising a question as to whether these genes display aberrations in humans. Sequencing analysis of the exons of the *CaMKIIα* gene in 80 blood samples from patients with dementia yielded two mutations at residues 1182 and 1197 (AAG^{1182} > AAC^{1182}, K323N and AAG^{1197} > GAG^{1197}, K328E) (Figure 6A), but no mutations were identified in 80 normal control samples. K323 and K328 sites are found in various species (Figure 6B). CaMKIIα K323N and K328E mutants were used to evaluate T286 phosphorylation, and we found that these two mutations restrain T286 phosphorylation (Figures 6C, lanes 6 and 7 versus lane 1, and 6D). Moreover, S-tag pull-down assays showed that CaMKIIα K323N and K328E mutants fail to interact with PTENα or NR2B (Figures 6C, lanes 6 and 7 versus lane 1, and 6E). In addition, both CaMKIIα mutants K323N and K328E showed weak binding ability with CaM (Figure 6F, lanes 3 and 4 versus lane 2). These results indicate that CaMKIIα mutations inhibit CaMKII phosphorylation at T286 and CaM binding, resulting in subsequent disruption of PTENα-CaMKIIα-NR2B signaling in patients with dementia.

DISCUSSION

Using a mouse model with PTENα-specific deletion, we demonstrate that PTENα regulates hippocampal LTP, fear-conditioned memory, and spatial learning through modulation of CaMKII signaling.

PTENα shares mRNA identical with PTEN (Liang et al., 2014), and we generated a mouse line in which there is specific knock out of PTENα without alteration of PTEN expression to evaluate the role of PTENα. Western blots showed an obvious band below PTENα, which was recognized by general PTEN antibody, raising the possibility this band represents another PTEN isoform. However, this undefined band was unchanged in our PTENα knockout mouse model. This PTENα mouse model thus allowed direct evaluation of specific PTENα function without interference from other isoforms.

Using a PTEN antibody that recognizes both PTEN and PTENα, we found PTENα expression is relatively low compared to PTEN. This raised a question as to how PTENα deletion, which eliminates only a small fraction of PTEN protein overall, can result in a phenotype which is based on regulation of the very abundant protein CaMKIIα. PTENα functions as a phosphatase of CaMKIIα, and phosphorylation of T305/306 and T337 are involved in the PTENα and CaMKIIα interaction. This indicates that PTENα/CaMKIIα binding is likely a transient substrate interaction, allowing one PTENα molecule to act on several CaMKIIα molecules. Moreover, PTENα acts on T305/306- or T337-phosphorylated CaMKIIα, the expression level of which is in total less than that of total CaMKIIα. As an additional important feature of this pathway, our data demonstrate PTENα binds to the CaMKII holoenzyme. Therefore, when two neighboring subunits of CaMKII simultaneously bind Ca^{2+}/CaM, autophosphorylation at T286 occurs (Hudmon and Schulman, 2002b), implying PTENα dephosphorylation of one or two subunits at T305/306 enables all other subunits within the holoenzyme to be activatable, despite the fact these other subunits are T305/306-phosphorylated. Based on our analysis overall, it is reasonable that the phenotype which results from PTENα loss is mediated by CaMKII dysfunction.

Functions of "PTEN" in the nervous system are heterogeneous (Sperow et al., 2012; Takeuchi et al., 2013; Wang et al., 2006). For example, deletion of the PTEN gene affects multiple forms of hippocampal synaptic plasticity including LTP throughout postnatal development. In contrast, only NMDAR-dependent long-term depression (LTD) is affected in acute blockage of PTEN activity in hippocampal slices (Jurado et al., 2010; Knafo and Esteban, 2017). In our study, the role of PTENα in LTP was identified with a PTENα-deficient mouse model. The effects of PTENα knockout on CaMKII were obtained from experiments performed with naive animals, demonstrating that PTENα affects "basal" CaMKII phosphorylation and maintains CaMKII in a state which is competent to induce LTP (Coultrap and Bayer, 2012). Moreover, PTENα expression is relatively

Figure 5. PTENα Reintroduced into the Hippocampus of *Pten*$\alpha^{mu/mu}$ Mice Reverses Spatial Learning Deficits

(A) Schematic of the lentivirus construct of human PTENα with WPRE-EGFP.

(B) Illustration of the injection region of the mouse brain. The left is white light image, and the right is stereo imaging.

(C) Representative image of GFP expression in dentate gyrus (DG) and CA1 of Lenti-GFP- and Lenti-PTENα-GFP-injected mice.

(D and E) Western blot and quantitative analysis of protein levels in hippocampal lysates from Lenti-PTENα-GFP-injected *Pten*$\alpha^{mu/mu}$ mice, Lenti-GFP-injected *Pten*$\alpha^{mu/mu}$ mice, and Lenti-GFP-injected *Pten*$\alpha^{+/+}$ mice. (D) Western blot of GFP, phospho-CaMKIIα$^{T305/306}$, phospho-CaMKIIα^{T286}, phospho-AKT^{S473}, and AKT protein levels. (E) Mean fold difference ± SEM of phospho-CaMKIIα$^{T305/306}$ and phospho-CaMKIIα^{T286} protein levels (comparison with Lenti-GFP-injected *Pten*$\alpha^{+/+}$ mice). Protein levels were normalized with CaMKIIα, a significant difference was observed only in Lenti-GFP-injected *Pten*$\alpha^{mu/mu}$ mice (n = 4, each group).

(F–H) Data from the Morris water maze for Lenti-PTENα-GFP-injected *Pten*$\alpha^{mu/mu}$ mice (n = 10), Lenti-GFP-injected *Pten*$\alpha^{mu/mu}$ mice (n = 9), and Lenti-GFP-injected *Pten*$\alpha^{+/+}$ mice (n = 8). (F) Design of Morris water maze (upper panel); the performance of Lenti-PTENα-GFP-injected *Pten*$\alpha^{mu/mu}$ mice was consistent with Lenti-GFP-injected *Pten*$\alpha^{+/+}$ mice (lower panel). (G) Lenti-PTENα-GFP-injected *Pten*$\alpha^{mu/mu}$ mice and Lenti-GFP-injected *Pten*$\alpha^{+/+}$ mice performed better than Lenti-GFP-injected *Pten*$\alpha^{mu/mu}$ mice in the probe trail on day 11. T, targeted quadrant; R, right quadrant; O, opposite quadrant; L, left quadrant. (H) Morris water maze testing of Lenti-GFP-injected *Pten*$\alpha^{+/+}$ mice (n = 8 mice), Lenti-GFP-injected *Pten*$\alpha^{mu/mu}$ mice (n = 9 mice), and Lenti-PTENα-GFP-injected *Pten*$\alpha^{mu/mu}$ mice (n = 10 mice). The average speed (cm/s) of each group showed no significant difference.

*p < 0.05, **p < 0.01, and ***p < 0.001. The data represent mean ± SEM. See also Figure S6.

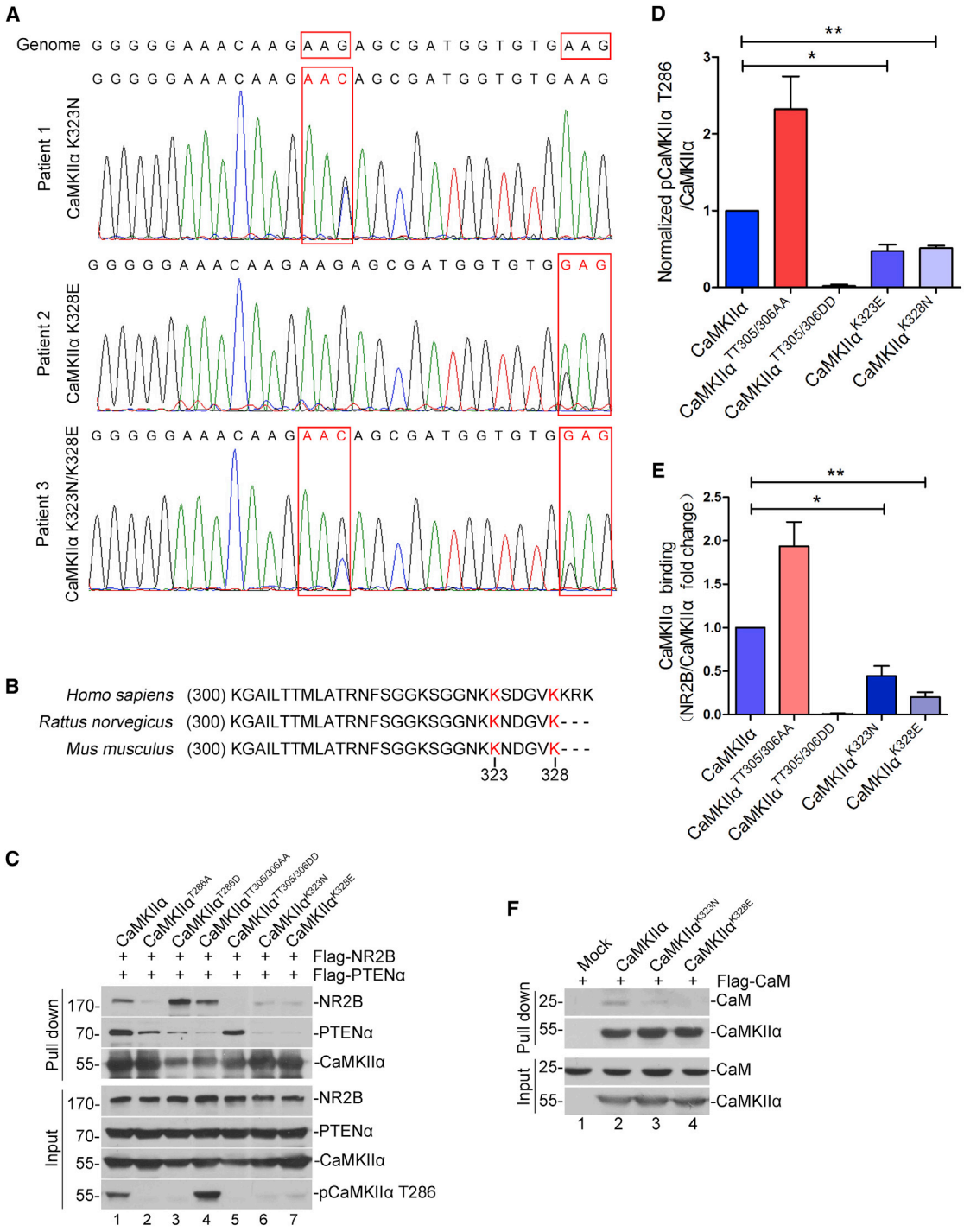

Figure 6. Mutations of CaMKIIα Were Identified in Patients with Dementia

(A) Sequencing analysis of blood samples. Genomic DNA from blood samples was extracted and used as a template for amplifying the exons of *CaMKIIα* with specific primers, and the products of amplification were subjected to sequencing analysis. 3 out of 80 patients had CaMKIIα mutations. Patient 1: AAG^{1182} > AAC^{1182}, K323N; patient 2: AAG^{1197} > GAG^{1197}, K328E; patient 3: AAG^{1182} > AAC^{1182}, K323N and AAG^{1197} > GAG^{1197}, K328E. There were no mutations found in 80 normal blood samples.

(B) CaMKIIα K323 and K328 sites (red) in different species (*Homo sapiens*, *Rattus norvegicus*, and *Mus musculus*).

(legend continued on next page)

low, while CaMKIIα is very abundant, indicating PTENα cannot affect CaMKII acutely during LTP induction. Most important, acute inhibition of PTEN function has no effect on LTP (Knafo and Esteban, 2017), which excludes the possibility that PTENα has an acute effect on LTP. We therefore think that it is most accurate to describe the regulatory effect of PTENα on LTP as "predisposing" rather than as an acute effect. In fact, the acute function of PTEN (including canonical PTEN and its isoforms) in LTD is likely due to the role PTENα plays in LTD. However, there is less expression of PTENα as compared to total PTEN, and any function of PTENα would require something that is unique to PTENα. Indeed, our data showed an increase in basal T305/306 phosphorylation induced by PTENα deletion, which would be expected to limit the induction of T286 phosphorylation during LTD stimulation. Moreover, CaMKII and its T286 autophosphorylation have been described as requirements for LTD (Coultrap et al., 2014). Thus, it seems likely that PTENα acts on LTD through CaMKII, while on the other hand it seems unlikely that PTENα contributes to LTD through the same mechanism, which is already mediated by the more highly expressed PTEN.

The PTENα-CaMKIIα-NR2B axis we identify in this study plays a critical role in learning and memory regulation, and its disruption by CaMKIIα mutation is likely a factor in the development of dementia in humans. Learning and memory phenotypes in PTENα-deficient mice are identical to those in CaMKIIα mutant mice (CaMKIIα T286A and CaMKIIα T305D) (Elgersma et al., 2002; Giese et al., 1998). Moreover, NR2B L1298A/R1300Q mutant mice display defects in memory consolidation (Halt et al., 2012). These studies emphasize the importance of these three molecules in learning and memory. CaMKIIα K323N and K328E are two mutations that are found only in patients with dementia and not in normal controls. Here, we simply wish to observe that these two mutations inhibit T286 phosphorylation and impair the binding of CaMKIIα with both PTENα and NR2B, and the exact mechanism underlying this process will require further study.

Our data demonstrate a role PTENα plays in molecular neural function. We have reported that PTENα modulates hippocampal LTP, together with contextual fear memory and spatial learning through regulation of CaMKII/NR2B signaling. Recognition of PTENα function in the brain furthers understanding of the complexity of the PTEN family in neural physiologic and pathologic processes. The findings in this study have the potential to pave the way for molecular diagnosis and therapy of neurological disorders.

EXPERIMENTAL PROCEDURES

PTENα-Specific Knockout Mouse Model

To generate *Pten*$\alpha^{mu/mu}$ mice, mouse embryonic stem cells (ESCs) were electroporated with a knockin-targeting construct designed to replace 347CTG and 362CTG of the PTEN gene with GGA. Animals were group housed in a climate controlled animal facility (22 ± 2°C), maintained on a 12 hr light/dark cycle, and fed ad libitum. Both male and female mice were used for biochemical experiments at 2–3 months of age. Only male mice were used for behavioral and electrophysiological experiments. All procedures followed the Peking University Guidelines for "Using Animals in Intramural Research" and were approved by the Animal Care and Use Committee of Peking University. For details, see Supplemental Experimental Procedures.

S-Tag Pull-Down Assay

HEK293T cells transfected with various plasmids or mice cortex tissue were lysed in NP-40 buffer (150 mM NaCl, 2 mM EDTA, 50 mM Tris-HCl, 0.5% NP-40, and protease inhibitor PMSF). Cell lysates were incubated with S-protein beads (Novagen) for 2 hr at 4°C, and precipitants were washed three times with NP-40 buffer (150 mM NaCl, 2 mM EDTA, 50 mM Tris-HCl, 0.5% NP-40, and PMSF) and subjected to NuPAGE 4%–12% gels (Invitrogen) and were then visualized with Coomassie Brilliant Blue staining (Bio-Rad) or subjected to immunoblot analysis with specific antibodies. Potential interacting proteins were evaluated with mass spectrum analysis.

Phosphatase Assay and In Vitro Binding

Purified phosphorylated CaMKIIα protein from transfected HEK293T cells was incubated with or without purified PTENα^{FL}, PTENα$^{N\text{-}ter}$, or PTENα$^{\Delta N\text{-}ter}$ in appropriate buffer. Reaction products were detected by mass spectrometry analysis or immunoblots. For details, see Supplemental Experimental Procedures.

Morris Water Maze

In the visual, hippocampal-independent version of the task, male mice were trained with three trials/day. A training protocol of three trials/day was used in the acquisition phase of the hidden platform version of the maze. Escape latencies were plotted against the results on the day of the experiment. Probe trials, during which the platform was removed from the maze, lasted 1 min. The quadrant exploration time was evaluated. For details, see Supplemental Experimental Procedures.

Contextual Fear Conditioning

Male mice were placed in the chamber for 3 min and received a mild footshock (0.75 mA for 2 s) after 150 s. Conditioning was tested 24 hr later in the same chamber, in a test for 5 min. Freezing was assessed using an automated procedure (Elgersma et al., 2002).

Electrophysiology

All electrophysiological experiments were performed with *Pten*$\alpha^{+/+}$ and *Pten*$\alpha^{mu/mu}$ male mice of 6 to 8 weeks old. Recordings were acquired with MultiClamp 700B and Digidtata 1440A (Molecular Devices). Series resistance were monitored during recordings and the data were excluded from analysis, if the series resistance changed >20% from control levels (15–30 MΩ). Data were analyzed with Clampfit 10 (Molecular Devices). For details, see Supplemental Experimental Procedures.

Statistical Analysis

Densitometric quantification of immunoblotting was performed using Quantity One software. Prism GraphPad software v5.01 was used for statistical analysis. Paired data were evaluated with the Student's t test, and error bars represent SEM. The data from behavioral analysis were evaluated with the two-tailed unpaired t test. The electrophysiology data were analyzed with two-tailed unpaired t test and two-way ANOVA. All data

(C) HEK293T cells were co-transfected to express S-tagged CaMKIIα, CaMKIIα$^{TT305/306AA}$, CaMKIIα$^{TT305/306DD}$, CaMKIIα^{T286A}, CaMKIIα^{T286D}, CaMKIIα^{K323N}, or CaMKIIα^{K328E} with FLAG-PTENα and FLAG-NR2B. Cell lysates were then precipitated with S-protein beads and subjected to immunoblotting with anti-NR2B, anti-FLAG, or anti-HA antibodies.

(D and E) Quantitative analysis of phosphorylation of CaMKIIα mutants at the T286 site (D) and CaMKIIα mutant-associated NR2B (E) (n = 3 replicates).

(F) HEK293T cells were co-transfected with S-tagged CaMKIIα, CaMKIIα^{K323N}, and CaMKIIα^{K328E}, with FLAG-CaM. Cell lysates were pulled down with S-protein beads and analyzed by immunoblot with anti-FLAG and anti-HA antibodies.

*p < 0.05, **p < 0.01, and ***p < 0.001. The data represent mean ± SEM.

are presented as mean ± SEM. p values of 0.05 or less were considered statistically significant.

SUPPLEMENTAL INFORMATION

Supplemental Information includes Supplemental Experimental Procedures, six figures, and two tables and can be found with this article online at http://dx.doi.org/10.1016/j.celrep.2017.05.088.

AUTHOR CONTRIBUTIONS

Y.Y. and P.W. conceived the study and designed the major experiments. P.W. performed experiments in behavioral examination, S-tag pull-down, phosphatase assay, and protein evaluation and analyzed the data. F.M. performed the electrophysiological experiments. J.H. performed behavioral examination, plasmid construction, and protein interaction related experiments. M.Z. generated the *Pten*α mutant mice. H.Q. performed immunoprecipitation experiments. X.C. was in charge of mouse management. R.L. performed the open field test. The manuscript was written by P.W., F.M., M.A.M., and Y.Y.

ACKNOWLEDGMENTS

We thank Ling Liang for protein purification, Chang Song and Yizhang Zhu for data analysis, and Xuyang Zhao and Juntuo Zhou for mass spectrum technical assistance. This study was supported by the following grants to Y.Y., including the National Natural Science Foundation of China (key grants 81430056, 31420103905, and 81372491), National Key Research and Development Program of China (grant 2016YFA0500302), Beijing Natural Science Foundation (key grant 7161007), and the Lam Chung Nin Foundation for Systems Biomedicine.

Received: January 16, 2017
Revised: April 13, 2017
Accepted: May 25, 2017
Published: June 20, 2017

REFERENCES

Backman, S.A., Stambolic, V., Suzuki, A., Haight, J., Elia, A., Pretorius, J., Tsao, M.S., Shannon, P., Bolon, B., Ivy, G.O., and Mak, T.W. (2001). Deletion of Pten in mouse brain causes seizures, ataxia and defects in soma size resembling Lhermitte-Duclos disease. Nat. Genet. *29*, 396–403.

Barcomb, K., Buard, I., Coultrap, S.J., Kulbe, J.R., O'Leary, H., Benke, T.A., and Bayer, K.U. (2014). Autonomous CaMKII requires further stimulation by Ca2+/calmodulin for enhancing synaptic strength. FASEB J. *28*, 3810–3819.

Bayer, K.U., LeBel, E., McDonald, G.L., O'Leary, H., Schulman, H., and De Koninck, P. (2006). Transition from reversible to persistent binding of CaMKII to postsynaptic sites and NR2B. J. Neurosci. *26*, 1164–1174.

Buard, I., Coultrap, S.J., Freund, R.K., Lee, Y.S., Dell'Acqua, M.L., Silva, A.J., and Bayer, K.U. (2010). CaMKII "autonomy" is required for initiating but not for maintaining neuronal long-term information storage. J. Neurosci. *30*, 8214–8220.

Chao, L.H., Stratton, M.M., Lee, I.H., Rosenberg, O.S., Levitz, J., Mandell, D.J., Kortemme, T., Groves, J.T., Schulman, H., and Kuriyan, J. (2011). A mechanism for tunable autoinhibition in the structure of a human Ca2+/calmodulin- dependent kinase II holoenzyme. Cell *146*, 732–745.

Colbran, R.J. (1993). Inactivation of Ca2+/calmodulin-dependent protein kinase II by basal autophosphorylation. J. Biol. Chem. *268*, 7163–7170.

Coultrap, S.J., and Bayer, K.U. (2012). CaMKII regulation in information processing and storage. Trends Neurosci. *35*, 607–618.

Coultrap, S.J., Buard, I., Kulbe, J.R., Dell'Acqua, M.L., and Bayer, K.U. (2010). CaMKII autonomy is substrate-dependent and further stimulated by Ca2+/calmodulin. J. Biol. Chem. *285*, 17930–17937.

Coultrap, S.J., Freund, R.K., O'Leary, H., Sanderson, J.L., Roche, K.W., Dell'Acqua, M.L., and Bayer, K.U. (2014). Autonomous CaMKII mediates both LTP and LTD using a mechanism for differential substrate site selection. Cell Rep. *6*, 431–437.

Elgersma, Y., Fedorov, N.B., Ikonen, S., Choi, E.S., Elgersma, M., Carvalho, O.M., Giese, K.P., and Silva, A.J. (2002). Inhibitory autophosphorylation of CaMKII controls PSD association, plasticity, and learning. Neuron *36*, 493–505.

Erickson, J.R., Joiner, M.L., Guan, X., Kutschke, W., Yang, J., Oddis, C.V., Bartlett, R.K., Lowe, J.S., O'Donnell, S.E., Aykin-Burns, N., et al. (2008). A dynamic pathway for calcium-independent activation of CaMKII by methionine oxidation. Cell *133*, 462–474.

Gardoni, F., Schrama, L.H., Kamal, A., Gispen, W.H., Cattabeni, F., and Di Luca, M. (2001). Hippocampal synaptic plasticity involves competition between Ca2+/calmodulin-dependent protein kinase II and postsynaptic density 95 for binding to the NR2A subunit of the NMDA receptor. J. Neurosci. *21*, 1501–1509.

Giese, K.P., Fedorov, N.B., Filipkowski, R.K., and Silva, A.J. (1998). Autophosphorylation at Thr286 of the alpha calcium-calmodulin kinase II in LTP and learning. Science *279*, 870–873.

Halt, A.R., Dallapiazza, R.F., Zhou, Y., Stein, I.S., Qian, H., Juntti, S., Wojcik, S., Brose, N., Silva, A.J., and Hell, J.W. (2012). CaMKII binding to GluN2B is critical during memory consolidation. EMBO J. *31*, 1203–1216.

Hopkins, B.D., Fine, B., Steinbach, N., Dendy, M., Rapp, Z., Shaw, J., Pappas, K., Yu, J.S., Hodakoski, C., Mense, S., et al. (2013). A secreted PTEN phosphatase that enters cells to alter signaling and survival. Science *341*, 399–402.

Hudmon, A., and Schulman, H. (2002a). Neuronal CA2+/calmodulin-dependent protein kinase II: the role of structure and autoregulation in cellular function. Annu. Rev. Biochem. *71*, 473–510.

Hudmon, A., and Schulman, H. (2002b). Structure-function of the multifunctional Ca2+/calmodulin-dependent protein kinase II. Biochem. J. *364*, 593–611.

Huttlin, E.L., Jedrychowski, M.P., Elias, J.E., Goswami, T., Rad, R., Beausoleil, S.A., Villén, J., Haas, W., Sowa, M.E., and Gygi, S.P. (2010). A tissue-specific atlas of mouse protein phosphorylation and expression. Cell *143*, 1174–1189.

Jurado, S., Benoist, M., Lario, A., Knafo, S., Petrok, C.N., and Esteban, J.A. (2010). PTEN is recruited to the postsynaptic terminal for NMDA receptor-dependent long-term depression. EMBO J. *29*, 2827–2840.

Kerchner, G.A., and Nicoll, R.A. (2008). Silent synapses and the emergence of a postsynaptic mechanism for LTP. Nat. Rev. Neurosci. *9*, 813–825.

Kessels, H.W., and Malinow, R. (2009). Synaptic AMPA receptor plasticity and behavior. Neuron *61*, 340–350.

Knafo, S., and Esteban, J.A. (2017). PTEN: local and global modulation of neuronal function in health and disease. Trends Neurosci. *40*, 83–91.

Krapivinsky, G., Medina, I., Krapivinsky, L., Gapon, S., and Clapham, D.E. (2004). SynGAP-MUPP1-CaMKII synaptic complexes regulate p38 MAP kinase activity and NMDA receptor-dependent synaptic AMPA receptor potentiation. Neuron *43*, 563–574.

Kwon, C.H., Zhu, X., Zhang, J., Knoop, L.L., Tharp, R., Smeyne, R.J., Eberhart, C.G., Burger, P.C., and Baker, S.J. (2001). Pten regulates neuronal soma size: a mouse model of Lhermitte-Duclos disease. Nat. Genet. *29*, 404–411.

Lee, Y.S., and Silva, A.J. (2009). The molecular and cellular biology of enhanced cognition. Nat. Rev. Neurosci. *10*, 126–140.

Leonard, A.S., Lim, I.A., Hemsworth, D.E., Horne, M.C., and Hell, J.W. (1999). Calcium/calmodulin-dependent protein kinase II is associated with the N-methyl-D-aspartate receptor. Proc. Natl. Acad. Sci. USA *96*, 3239–3244.

Leonard, A.S., Bayer, K.U., Merrill, M.A., Lim, I.A., Shea, M.A., Schulman, H., and Hell, J.W. (2002). Regulation of calcium/calmodulin-dependent protein kinase II docking to N-methyl-D-aspartate receptors by calcium/calmodulin and alpha-actinin. J. Biol. Chem. *277*, 48441–48448.

Liang, H., He, S., Yang, J., Jia, X., Wang, P., Chen, X., Zhang, Z., Zou, X., McNutt, M.A., Shen, W.H., and Yin, Y. (2014). PTENα, a PTEN isoform translated through alternative initiation, regulates mitochondrial function and energy metabolism. Cell Metab. *19*, 836–848.

Lisman, J., Schulman, H., and Cline, H. (2002). The molecular basis of CaMKII function in synaptic and behavioural memory. Nat. Rev. Neurosci. *3*, 175–190.

Lu, C.S., Hodge, J.J., Mehren, J., Sun, X.X., and Griffith, L.C. (2003). Regulation of the Ca2+/CaM-responsive pool of CaMKII by scaffold-dependent autophosphorylation. Neuron *40*, 1185–1197.

Lugo, J.N., Smith, G.D., Arbuckle, E.P., White, J., Holley, A.J., Floruta, C.M., Ahmed, N., Gomez, M.C., and Okonkwo, O. (2014). Deletion of PTEN produces autism-like behavioral deficits and alterations in synaptic proteins. Front. Mol. Neurosci. *7*, 27.

Malenka, R.C., and Bear, M.F. (2004). LTP and LTD: an embarrassment of riches. Neuron *44*, 5–21.

Martin, S.J., Grimwood, P.D., and Morris, R.G. (2000). Synaptic plasticity and memory: an evaluation of the hypothesis. Annu. Rev. Neurosci. *23*, 649–711.

O'Leary, H., Liu, W.H., Rorabaugh, J.M., Coultrap, S.J., and Bayer, K.U. (2011). Nucleotides and phosphorylation bi-directionally modulate Ca2+/calmodulin-dependent protein kinase II (CaMKII) binding to the N-methyl-D-aspartate (NMDA) receptor subunit GluN2B. J. Biol. Chem. *286*, 31272–31281.

Rellos, P., Pike, A.C., Niesen, F.H., Salah, E., Lee, W.H., von Delft, F., and Knapp, S. (2010). Structure of the CaMKIIdelta/calmodulin complex reveals the molecular mechanism of CaMKII kinase activation. PLoS Biol. *8*, e1000426.

Sanhueza, M., Fernandez-Villalobos, G., Stein, I.S., Kasumova, G., Zhang, P., Bayer, K.U., Otmakhov, N., Hell, J.W., and Lisman, J. (2011). Role of the CaMKII/NMDA receptor complex in the maintenance of synaptic strength. J. Neurosci. *31*, 9170–9178.

Shen, K., and Meyer, T. (1999). Dynamic control of CaMKII translocation and localization in hippocampal neurons by NMDA receptor stimulation. Science *284*, 162–166.

Silva, A.J., Paylor, R., Wehner, J.M., and Tonegawa, S. (1992). Impaired spatial learning in alpha-calcium-calmodulin kinase II mutant mice. Science *257*, 206–211.

Sperow, M., Berry, R.B., Bayazitov, I.T., Zhu, G., Baker, S.J., and Zakharenko, S.S. (2012). Phosphatase and tensin homologue (PTEN) regulates synaptic plasticity independently of its effect on neuronal morphology and migration. J. Physiol. *590*, 777–792.

Strack, S., and Colbran, R.J. (1998). Autophosphorylation-dependent targeting of calcium/ calmodulin-dependent protein kinase II by the NR2B subunit of the N-methyl- D-aspartate receptor. J. Biol. Chem. *273*, 20689–20692.

Strack, S., McNeill, R.B., and Colbran, R.J. (2000). Mechanism and regulation of calcium/calmodulin-dependent protein kinase II targeting to the NR2B subunit of the N-methyl-D-aspartate receptor. J. Biol. Chem. *275*, 23798–23806.

Takeuchi, K., Gertner, M.J., Zhou, J., Parada, L.F., Bennett, M.V., and Zukin, R.S. (2013). Dysregulation of synaptic plasticity precedes appearance of morphological defects in a Pten conditional knockout mouse model of autism. Proc. Natl. Acad. Sci. USA *110*, 4738–4743.

Wang, Y., Cheng, A., and Mattson, M.P. (2006). The PTEN phosphatase is essential for long-term depression of hippocampal synapses. Neuromolecular Med. *8*, 329–336.